RAP CONFERENCE PROCEEDINGS, VOL. 8, PP. 60–64, 2023
ISSN 2737-9973 (ONLINE) | DOI: 10.37392/RAPPROC.2023.13
RAP-PROCEEDINGS.ORG

IMAGE QUALITY IMPACT OF DIFFERENT PHOSPHOR ACTIVATOR MATERIALS IN Gd_2O_2S BASED EPID SYSTEMS

Marios K. Tzomakas[1*], Vasiliki Peppa[2], Antigoni Alexiou[2], Georgios Karakatsanis[2], Anastasios Episkopakis[3,4], Christos Michail[1], Ioannis Valais[1], George Fountos[1], Ioannis S. Kandarakis[1], Nektarios Kalyvas[1]

[1]Radiation Physics, Materials Technology and Biomedical Imaging Laboratory, Department of Biomedical Engineering, University of West Attica, Egaleo, Athens, Greece
[2]General Hospital of Athens Alexandra, Department of Radiotherapy, Athens, Greece
[3]Elekta, Athens, Greece
[4]Medical Physics Laboratory, Medical School, National and Kapodistrian University of Athens, Athens, Greece

Abstract. *In this work, the effect of the scintillator on EPIDs signal transfer properties was examined. Modulation Transfer Function, Signal Power Spectrum and Light Output were assessed by analytical models while radiation incidence was estimated by Monte Carlo techniques. The frequency dependent Contrast Transfer Function (CTF) of a Gd_2O_2S:Tb based EPID system was experimentally determined by imaging the QC3 phantom in an iViewGT™ R3.4.1 MV Portal Imaging system for 6MV, 2MU and 400 DR irradiation conditions. In addition, an approximation of experimental MTF was determined. The Eu activator showed the highest light output per incident photon. A more detailed study should include the effect of scatter on MTF and the determination of the experimental MTF through CTF.*

Keywords: *activator, EPID, evaluation, image, PenEasy, MTF, phantom, phosphor, QC3, scintillator*

1. INTRODUCTION

Electronic Portal Imaging Systems (EPIDs) are used in Radiotherapy treatment as part of the patient positioning verification check [1]-[7]. Previously published investigations have applied methods for EPID quality assurance and image evaluation based on measuring the Modulation Transfer Function (MTF), the Noise Power Spectrum (NPS), using specific phantoms and dedicated software [8]-[11]. Studies, are investigating various EPID issues such as the effects of external aluminum target beam of the LINAC on EPID, the effect of the irradiation beam size the effect of the detector layers and the use of EPID for dosimetry [1]-[13]. The theoretical and experimental evaluation of Gd_2O_2S granular phosphor properties as well as, the light emission efficiency of phosphor-based detectors in medical imaging have been reported in literature [13]-[23]. EPIDs use scintillator materials to convert the energy of absorbed ionizing photons to optical photons. Since an ionizing radiation photon can produce numerous optical photons with lower energy, the signal (photons) is amplified. In EPID systems a Gd_2O_2S:X based granular scintillator, is used where X is the activator [1], [3], [4], [7], [8]. The activator is responsible to provide the required energy levels for the optical emission decay. The Gd_2O_2S a material with density 7.34 g/cm3 and a 50% packing is customary combined with Tb activator. However, in X-ray imaging has also been studied combined with Eu and Pr activators as well [13]-[17], [21]. The activator role is crucial since it affects the energy and the number of the generated optical photons, which in turn affect the interactions of the optical photons inside the scintillator and their spatial distribution in the phosphor exit, thus affecting the system's imaging performance. In addition, the emitted optical spectra should match the sensitivity curves of the optical detectors, providing a high detecting efficiency, also known as spectral matching factor [13]-[23]. The aim of the present work was to investigate the effect of activator type on the signal transfer properties of EPIDs (spatial resolution, light emission efficiency of their scintillator, signal power, etc.). To this aim, parameters related to spatial resolution and light output, such as the Modulation Transfer Function (MTF), the Contrast Transfer Function (CTF) [11], [24], the number of emitted optical photons as well as the Signal Power Spectrum (SPS), were studied employing theoretical and experimental methods [11], [13], [18], [22], [25]. The effect of the activator was examined by considering three different ones, namely Tb, Eu and Pr. The spectral matching factor of the Gd2O2S host combined with Tb, Eu and Pr can be obtained from literature [13], [14], [16], [17].

2. MATERIALS AND METHODS

The PENELOPE based MC software package [26]-[29] was used to simulate x-ray beam incidence and energy deposition. A narrow cone beam geometry with

* mtzomakas@uniwa.gr

a cross section of 0.00053 cm² at 100 cm distance was considered. The beam was assumed to impinge on 1.8 cm Al in contact with 2 cm water equivalent phantom, simulating the bulk materials of QC3V EPID phantom assuming that for high energies water and plastic demonstrated similar radiation interaction properties [33]. At 160 cm distance a Gd_2O_2S based scintillator, as part of an EPID responsible for detecting X-rays was considered, with thickness 0.018 cm (Figure 1) [7], [8], [11]. The photon energy was 2 MeV. The energy deposition in Gd_2O_2S was determined and the corresponding MTF was calculated using an analytical model (1). The model is based on an analytical description of the optical photon generation in the scintillator and the light propagation to the output [15], [23], [25]. In this framework MTF was expressed as follows:

$$MTF(u)=\frac{\sum_i fE_{abs}\frac{n_c}{E_\lambda}Q_i(E)G_i(u)}{\sum_i fE_{abs}\frac{n_c}{E_\lambda}Q_i(E)G_i(0)} \quad (1)$$

where, f: number of photons, Q(E): fraction of energy absorbed in layer i, E_{abs}: Energy absorbed in Gd_2O_2S, n_C E_{abs}/E_λ gives the number of optical photons produced, *G(u)*: the spatial frequency distribution to the output of the photons generated in layer *i* given by [15], [23], [25]:

$$G_i(u)=\frac{\tau\rho_1(b+\tau\rho_0)e^{bi\Delta t}+\tau\rho_1(b-\tau\rho_0)e^{-bi\Delta t}}{(b+\tau\rho_0)(b+\tau\rho_1)e^{bT}-(b-\tau\rho_0)(b-\tau\rho_1)e^{-bT}} \quad (2)$$

with

$$b=\sqrt{\sigma^2+(2\pi u')^2} \quad (3)$$

where σ: reciprocal diffusion length (shows optical photon propagation and is affected by optical photon absorption and scattering), u: spatial frequency divided by the material's packing density, τ: inverse relaxation length (affected by the optical photons' absorption and scattering), ρ: reflection to output (0) or input (1), T: scintillator thickness [18], [25].

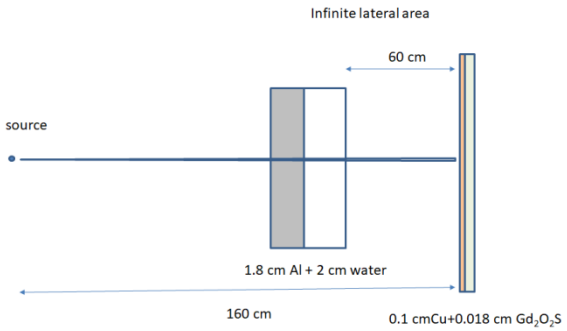

Figure 1. Monte Carlo experimental Set-up

Analytical calculations were performed for three different activators, i.e. Tb, Eu and Pr within a Gd_2O_2S powder phosphor host. The absorbed dose and 1D depth dose distribution were calculated in Gd_2O_2S using Peneasy software. Finally, the frequency dependent Contrast Transfer Function (CTF) of a Gd_2O_2S:Tb based EPID system was experimentally determined by imaging the QC3 phantom [19] in an iViewGT™ R3.4.1 MV Portal Imaging system for 6MV, 2MU and 400 DR irradiation conditions. A QC3 phantom was irradiated in an iViewGT™ R3.4.1 MV Portal Imaging system for 6MV, 2MU and 400 DR irradiation conditions. An approximated MTF (*aMTF*) was calculated by means of the Coltman formula [11], [24]:

$$MTF(f)=\frac{\pi}{4}\left[CTF(f)+\frac{CTF(3f)}{3}-\frac{CTF(5f)}{5}+\ldots\right] \quad (4)$$

with

$$CTF(f)=\frac{\mu_{max}(f)-\mu_{min}(f)}{\mu_{max}(f)+\mu_{min}(f)} \quad (5)$$

where $\mu_{max,min}$ corresponds to the min and max pixel value of a bar pattern image.

Finally, based on the theoretical MTF data, the Signal Power Spectrum, indicating the distribution of absolute signal in the spatial frequency domain, was calculated as follows:

$$SPS(u)=\left[Signal\times MTF(u)\right]^2 \quad (6)$$

where *Signal* corresponds to the light output, calculated through the equation (1), described by the denominator. The phosphor related parameters used are shown in Table 1 [13], [15], [16], [25], [30]-[32].

Table 1. The parameters of the three scintillator materials

	Gd_2O_2S:Tb	Gd_2O_2S:Eu	Gd_2O_2S:Pr
Vendor/ code	Derby Luminescence GD1016	Phosphor Technology UKL63/N-R1	Phosphor Technology UKL59/N-R3
E_λ	2.46 eV	1.99 eV	2.16 eV
n_C	0.1722	0.1194	0.108
σ	30 cm²/g	6.1 cm²/g	600 cm²/g
τ	1000 cm²/g	203.3 cm²/g	20000 cm²/g
$\rho_1=\rho_0$	1	1	1
T	0.018 cm	0.018 cm	0.018 cm
Grain size	7 μm	8 μm	8 μm
Activator	-	0.92%	1%

3. Results and Discussion

Figure 2 shows the 1D dose distribution with depth within the scintillator mass. The statistical uncertainties of the simulations were below 1.5%. In order to calculate the fraction of energy absorbed in each layer i, (Q_i) each energy bin per Δt was divided by the sum of Q_i when all energy bins are considered (Figure 2). The simulation presented in this work considers a narrow X-ray beam passing through slabs of different materials and the optical phenomena are described through an analytical formula. The size of the beam and the type of the materials and the thickness of the Cu sheet used, significantly affect the EPID response. In addition, the effect of the optical transport in the photodiode modifies the PSF of the system and subsequently the calculated MTF [3], [4].

It was found that the MTF of Gd_2O_2S:Tb phosphor was superior to that of Gd_2O_2S:Eu, having a value of approximately 0.51 at 24 lp/cm spatial frequency (Figure 3). The corresponding value for Gd_2O_2S:Eu at

24 lp/cm spatial frequency for the 0.018 cm thickness scintillator was 0.25. Pr activator exhibited the highest MTF, but the light output results were significantly inferior to the other phosphors making the use of Gd_2O_2S:Pr an impractical choice (Figure 4). If the optical data for the UFC version of Gd_2O_2S:Pr were available a significantly higher performance would be anticipated. The Eu activator showed the highest light output per incident photon. This result can be affected by the size and the shape of the grains of the scintillator materials. The signal power spectrum was calculated as the square of the nominator of theoretical MTF calculation formula.

Figure 5 shows data on SPS for the three materials. Eu produces the highest signal, up to 13380 (photons)^2. Tb has a significantly lower amount, approximately 3372 (photons)^2 and Pr has the lowest, nearly zero. The shapes of the curves are different in the sense that the Gd_2O_2S:Eu values roll off very fast, however being clearly higher than those of Gd_2O_2S:Tb, in the whole frequency range. The Eu activator showed medium values at very low frequencies, approximately 5000 (photons)^2. For higher spatial frequencies the values decrease exponentially.

The deviation in the experimental CTF was below 5% at 7.89 lp/cm spatial frequency (Figure 6). The corresponding normalized CTF value at 7.89 lp/cm was close to 0.25.

In Figure 7, the experimental (*aMTF*) is demonstrated. The difference between the theoretical MTF and the experimental *aMTF* are due to the effect of pixel sampling, the effect of scatter radiation and any software algorithms that are imposed in the image [6], [11].

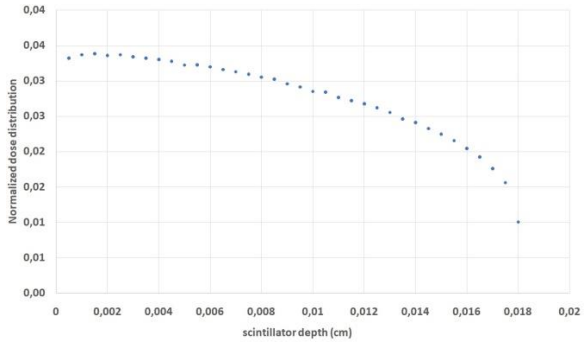

Figure 2. 1D dose distribution

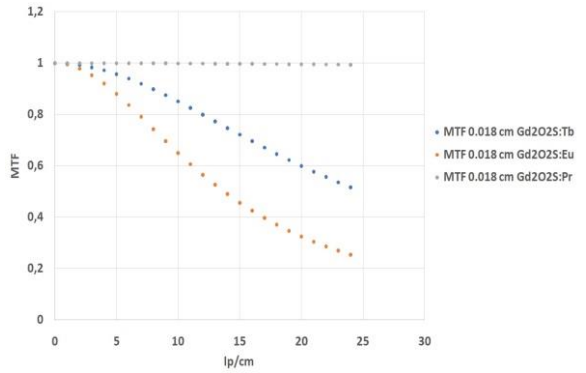

Figure 3. Theoretical MTFs of the three scintillator materials

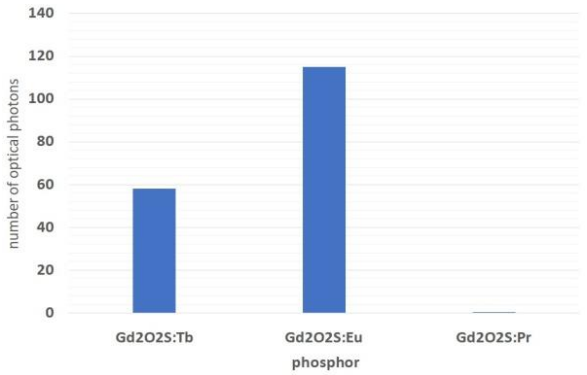

Figure 4. Signal in terms of light output for the scintillators under investigation

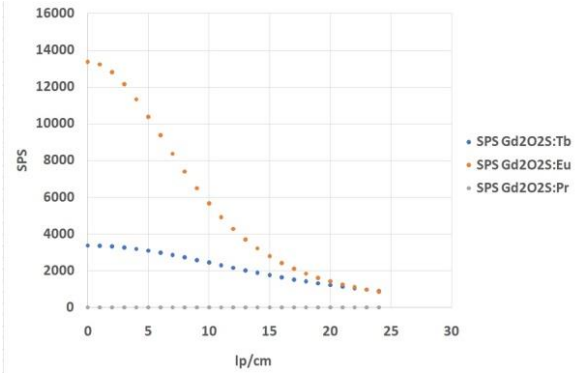

Figure 5. SPS of the three materials

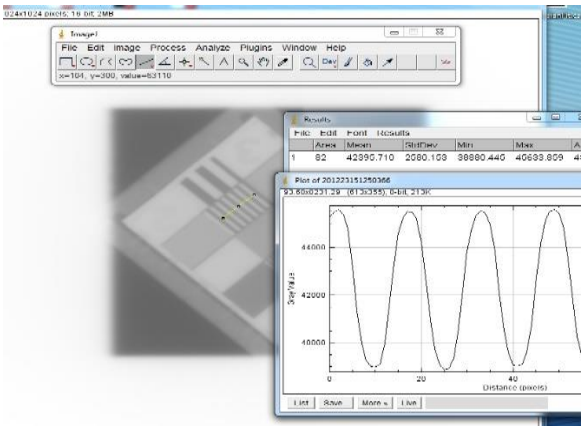

Figure 6. Experimental CTF calculation using QC3 phantom

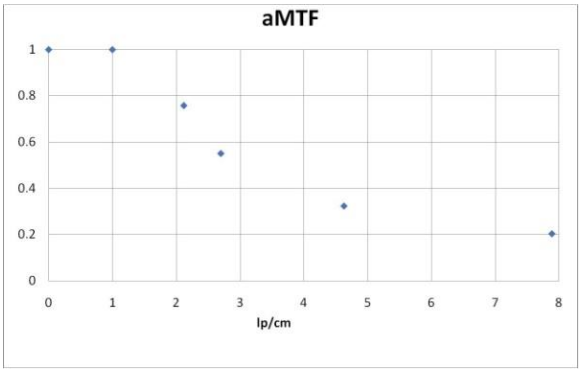

Figure 7. Experimental *aMTF*

The theoretically calculated MTF of Gd_2O_2S:Tb demonstrates higher values than the experimental one, for the available spatial frequencies 0 up to 8 lp/cm. The experimental MTF besides the scintillator incorporates the effect of pixel sampling and the effect of scatter radiation in the scintillator. The experimental MTF was measured by an irradiated image of a 6 MV X-ray spectrum, while the theoretical one was calculated by considering 2 MeV ionizing radiation, where 2 MeV is the average energy of the 6 MV photon spectrum.

Conclusion

The MTF and the signal transfer properties of a scintillator based EPID has been investigated by theoretical and experimental methods. It was found that Tb activator practically presents an optimum activator choice. A more detailed study should include the effect of scatter in MTF and the determination of the experimental MTF through CTF. The Pr activator provides the highest MTF, but practically zero signal. The Tb activator demonstrates higher MTF values than the Eu activator, mainly due to the optical photon propagation characteristics. The Tb activator demonstrates higher MTF values than the Eu activator. The Eu activator shows the highest light output and signal power spectrum (SPS). A comparison with the experimental MTF, should also consider the effects of pixel size and scatter in the scintillator. Finally a future investigation may include the UFC version Gd_2O_2S:Pr and Gd_2O_2S: (Pr, Ce, F) phosphor performance characteristics. In addition, different component layers and thicknesses may be considered in EPID setup.

References

1. F. Cremers et al., "Performance of electronic portal imaging devices EPID used in radiotherapy: Image quality and dose measurements," *Med. Phys.*, vol. 31, no. 5, pp. 985 – 996, May 2004. DOI: 10.1118/1.1688212 PMid: 15191282
2. J. Seco, B. Clasie, M. Partridge, "Review on the characteristics of radiation detectors for dosimetry and imaging," *Phys. Med. Biol.*, vol 59, no. 20, pp. R303 – R347, Oct. 2014. DOI: 10.1088/0031-9155/59/20/R303 PMid: 25229250
3. S. J. Blake et al., "Characterization of optical transport effects on EPID dosimetry using Geant4," *Med. Phys.*, vol. 40, no. 4, 041708, Apr. 2013. DOI: 10.1118/1.4794479 PMid: 23556878
4. H. Gustafsson, P. Vial, Z. Kuncic, C. Baldock, P. B. Greer, "EPID dosimetry: Effect of different layers of materials on absorbed dose response," *Med. Phys.*, vol. 36, no. 12, pp. 5665 – 5674, Dec. 2009. DOI: 10.1118/1.3245886 PMid: 20095279
5. N. Dogan et al., "AAPM Task Group Report 307: Use of EPIDs for Patient-Specific IMRT and VMAT QA," *Med. Phys.*, vol. 50, no. 8, pp. e865 – e903, Aug. 2023. DOI: 10.1002/mp.16536 PMid: 37384416
6. Chia-Lung Chien, X. Zhao, B. Guo, R. Zhang, "Technical note: Preprocessing of portal images to improve image quality of VMAT-CT," *Med. Phys.*, Sep. 2023. DOI: 10.1002/mp.16741 PMid: 37727132
7. L. E. Antonuk, "Electronic portal imaging devices: a review and historical perspective of contemporary technologies and research," *Phys. Med. Biol.*, vol. 47, no. 6, pp R31 – R65, Mar. 2002. DOI: 10.1088/0031-9155/47/6/201 PMid: 11936185
8. S. Y. Son et al., "Evaluation of Image Quality for Various Electronic Portal Imaging Devices in Radiation Therapy," *J. Radiol. Sci. Technol.*, vol. 38, no. 4, pp. 451 – 461, Dec. 2015. DOI: 10.17946/JRST.2015.38.4.16
9. I. J. Das et al., "A quality assurance phantom for electronic portal imaging devices," *J. Appl. Clin. Med. Phys.*, vol. 12, no. 2, pp. 39 1- 403, Feb. 2011. DOI: 10.1120/jacmp.v12i2.3350 PMid: 21587179 PMCid: PMC5718680
10. J. Baek, H. Kim, B. Kim, Y. Oh, H. Jang, "Assessment of portal image resolution improvement using an external aluminum target and polystyrene electron filter," *Radiat. Oncol.*, vol. 14, no. 1, 70, Apr. 2019. DOI: 10.1186/s13014-019-1274-4 PMid: 31023340 PMCid: PMC6485051
11. M. K. Tzomakas et al., "A phantom based evaluation of the clinical imaging performance of electronic portal imaging devices," *Helyion*, vol. 9, no. 10, e21116, Oct. 2023. DOI: 10.1016/j.heliyon.2023.e21116 PMid: 37916082 PMCid: PMC10616349
12. Z. Zarrini-Monfared, S. Karbasi, A. Zamani, M. A. Mosleh-Shirazi, "Full modulation transfer functions of thick parallel- and focused-element scintillator arrays obtained by a Monte Carlo optical transport model," *Med. Phys.*, vol. 50, no. 6, pp. 3651 – 3660, Oct. 2023. DOI: 10.1002/mp.16306 PMid: 36779548
13. S. David et al., "Evaluation of Gd_2O_2S:Pr granular phosphor properties for X-ray mammography imaging," *J. Lumin.*, vol. 169, pt. B, pp. 706 – 710, Jan. 2016. DOI: 10.1016/j.jlumin.2015.01.044
14. C. M. Michail et al., "Evaluation of the Red Emitting Gd_2O_2S:Eu Powder Scintillator for Use in Indirect X-Ray Digital Mammography Detectors," *IEEE Trans. Nucl. Sci.*, vol. 58, no. 5, pp. 2503 – 2511, Oct. 2011. DOI: 10.1109/TNS.2011.2162002
15. C. M. Michail et al., "Experimental and Theoretical Evaluation of a High Resolution CMOS Based Detector Under X-Ray Imaging Conditions *IEEE Trans. Nucl. Sci.*, vol. 58, no. 1, pp 314 – 322, Feb. 2011. DOI: 10.1109/TNS.2010.2094206
16. C. M. Michail et al., "Light emission efficiency of Gd_2O_2S:Eu (GOS:Eu) powder screens under X-ray mammography conditions," *IEEE Trans. Nucl. Sci.*, vol. 55, no. 6, pp. 3703 – 3709, Dec. 2008. DOI: 10.1109/TNS.2008.2007562
17. C. M. Michail et al., "Light emission efficiency and imaging performance of Gd_2O_2S:Eu powder scintillator under x-ray radiography conditions," *Med. Phys.*, vol. 37, no. 7, pp. 3694 – 3703, Jul. 2010. DOI: 10.1118/1.3451113 PMid: 20831077
18. N. Kalyvas et al., "Studying the luminescence efficiency of Lu_2O_3:Eu nanophosphor material for digital X-ray imaging applications," *Appl. Phys. A*, vol. 106, no. 1, pp. 131 – 136, Jan. 2012. DOI: 10.1007/s00339-011-6640-5
19. I. E. Seferis et al., "On the response of a europium doped phosphor-coated CMOS digital imaging detector," *Nucl. Instrum. Methods Phys. Res. A*, vol. 729, pp. 307 – 315, Nov. 2013. DOI: 10.1016/j.nima.2013.06.107
20. I. E. Seferis et al., "Light emission efficiency and imaging performance of Lu_2O_3:Eu nanophosphor under X-ray radiography conditions: Comparison with Gd_2O_2S:Eu," *J. Lumin.*, vol. 151, pp. 229 – 234, Jul. 2014.

DOI: 10.1016/j.jlumin.2014.02.017
21. S. David et al., "Evaluation of powder/granular Gd_2O_2S:Pr scintillator screens in single photon counting mode under 140 keV excitation," *JINST*, vol 8, P01006, Jan. 2013.
DOI: 10.1088/1748-0221/8/01/P01006
22. C. Michail et al., "On the response of $GdAlO_3$:Ce powder scintillators," *J. Lumin.*, vol. 144, pp. 45 – 52, Dec. 2013.
DOI: 10.1016/j.jlumin.2013.06.041
23. I. S. Kandarakis, "Luminescence in medical image science," *J. Lumin.*, vol. 169, pp. 553 – 558, Nov. 2014.
DOI: 10.1016/j.jlumin.2014.11.009
24. N. B. Nill, *Conversion between sine wave and square wave spatial frequency response of an imaging system*, Rep. MTR 01B0000021, MITRE, Bedford (MA), USA, 2001.
Retrieved from:
https://www.mitre.org/sites/default/files/pdf/nill_conversion.pdf
Retrieved on: May 8, 2023
25. N. Kalyvas, P. Liaparinos, "Analytical and Monte Carlo comparisons on the optical transport mechanisms of powder phosphors," *Opt. Mater.*, vol. 88, pp. 396 – 405, Feb. 2019.
DOI: 10.1016/j.optmat.2018.12.006
26. J. Sempau, A. Badal, L. Brualla, "A PENELOPE-based system for the automated Monte Carlo simulation of clinacs and voxelized geometries-application to far-from-axis fields," *Med. Phys.*, vol. 38, no. 11, pp. 5887 – 5895, Nov. 2011.
DOI: 10.1118/1.3643029
PMid: 22047353
27. J. Sempau, E. Acosta, J. Baro, J. M. Fernández-Varea, F. Salvat, "An algorithm for Monte Carlo simulation of coupled electron-photon transport," *Nucl. Instrum. Methods Phys. Res. B*, vol. 132, no. 3, pp. 377 – 390, Nov. 1997.
DOI: 10.1016/S0168-583X(97)00414-X
28. J. Baró, J. Sempau, J. M. Fernández-Varea, F. Salvat, "PENELOPE: An algorithm for Monte Carlo simulation of the penetration and energy loss of electrons and positrons in matter," *Nucl. Instrum. Methods Phys. Res. B*, vol. 100, no. 1, pp. 31 – 46, May 1995.
DOI: 10.1016/0168-583X(95)00349-5
29. F. Salvat, *PENELOPE: A code system for Monte Carlo simulation of electron and photon transport*, OECD Nuclear Energy Agency, Issy-les-Moulineaux, France, 2015.
30. A. De Martinis et al., "Luminescence and Structural Characterization of Gd2O2S Scintillators Doped with Tb3+, Ce3+, Pr3+ and F for Imaging Applications," *Crystals*, vol. 12, no. 6, 854, Jun. 2022.
DOI: 10.3390/cryst12060854
31. P. Liaparinos et al., "Grain Size Distribution Analysis of Different Activator Doped Gd2O2S Powder Phosphors for Use in Medical Image Sensors," *Sensors*, vol. 22, no. 22, 8702, Nov. 2022.
DOI: 10.3390/s22228702
PMid: 36433300
PMCid: PMC9695128
32. I. Kandarakis, D. Cavouras, "Experimental and theoretical assessment of the performance of Gd_2O_2S:Tb and La_2O_2S:Tb phosphors and Gd_2O_2S:Tb-La_2O_2S:Tb mixtures for X-ray imaging," *Eur. Radiol.*, vol. 11, no. 6, pp. 1083 – 1091, May 2001.
DOI: 10.1007/s003300000715
PMid: 11419159
33. R. Nowotny, *XMuDat: Photon Attenuation Data on PC Version 1.0.1*, Rep. IAEA-NDS-195, IAEA, Vienna, Austria, 1998.
Retrieved from:
https://nds.iaea.org/publications/nds/iaea-nds-0195/
Retrieved on: May 8, 2023